

Energy dependence of the relativistic impulse approximation for proton-nucleus elastic scattering

B. C. Clark and S. Hama

Department of Physics, The Ohio State University, Columbus, Ohio 43210

R. L. Mercer

Thomas Watson Research Laboratories, IBM Corporation, Yorktown Heights, New York 10598

L. Ray and G. W. Hoffmann

Department of Physics, University of Texas at Austin, Austin, Texas 78712

B. D. Serot

Institute of Theoretical Physics, Department of Physics, Stanford University, Stanford, California 94305

(Received 21 June 1983)

Results of relativistic and nonrelativistic impulse approximation calculations are compared for $p + {}^{40}\text{Ca}$ elastic scattering observables between 181 and 1040 MeV. At 400 MeV and above, the relativistic approach is superior, especially with regard to spin observables. Below 400 MeV, neither calculation agrees well with experiment.

NUCLEAR REACTIONS Energy dependence of the relativistic impulse approximation, Dirac phenomenology, invariant nucleon-nucleon amplitudes, nucleon-nucleus elastic scattering, $E_p = 181\text{--}1040$ MeV.

Recently, several authors have concluded that the general features of Dirac optical potential phenomenology¹ for intermediate energy proton + nucleus elastic scattering can be explained in terms of nucleon-nucleon (N-N) phenomenology by way of the relativistic impulse approximation (RIA).²⁻⁵ In this approach the Dirac optical potential is obtained by folding the N-N invariant scalar and vector amplitudes⁶ with appropriate scalar and vector densities for the target nucleus.^{3,4,7} For the relativistic case, this procedure has not been rigorously justified, but it is a reasonable extension of nonrelativistic (NR) multiple scattering theory,² and agreement with experiment establishes its pragmatic value. Here we examine the energy dependence of the RIA for $p + {}^{40}\text{Ca}$ elastic scattering from 181 to 1040 MeV. We contrast the relativistic and NR IA predictions and also compare the RIA with Dirac phenomenology.

For spin saturated target nuclei, the Dirac optical potential in the IA (Refs. 2-4 and 8) has contributions from scalar, vector, and tensor invariant amplitudes; however, by far the largest contributions arise from the scalar and vector terms. In this case,

$$U_{\text{opt}}(q) = -\frac{4\pi ik}{m} [F_S(q)\tilde{\rho}_S(q) + \gamma^0 F_V(q)\tilde{\rho}_V(q)] , \quad (1)$$

where k is the proton-nucleus center-of-momentum (c.m.) wave number, q is the momentum transfer, $\tilde{\rho}_S$ and $\tilde{\rho}_V$ are the scalar and vector densities, respectively, and F_S and F_V are the scalar and vector N-N invariant amplitudes. These latter quantities are obtained by expressing the N-N scattering matrix in the following covariant form⁶:

$$F(q) = F_S + F_V \gamma_1^\mu \gamma_2^\mu + F_P \gamma_1^5 \gamma_2^5 + F_A \gamma_1^5 \gamma_1^\mu \gamma_2^5 \gamma_2^\mu + F_T \sigma_1^{\mu\nu} \sigma_2^{\mu\nu} . \quad (2)$$

We computed $p + {}^{40}\text{Ca}$ elastic scattering observables at 181, 300, 400, 500, 613, 650, 800, and 1040 MeV for comparison with experiment. The relativistic Hartree calculations of Ref. 7 provided the proton and neutron, scalar and vector densities, while the invariant N-N amplitudes were obtained from the global energy independent phase shift solution, SP82, of Arndt.⁹ As in Ref. 4, the N-N invariant amplitudes were used directly, without approximation.

Predictions and data¹⁰⁻¹³ for 181, 400, 613, and 1040 MeV are shown in Figs. 1-4. The RIA results are indicated by solid curves, the NR, first order Kerman-McManus-Thaler (KMT) (Ref. 14) IA results by dashed curves. At 181 and 300 MeV, the RIA differential cross sections are too large and the analyzing powers are too small. At 400 MeV and above, both the differential cross sections and the analyzing powers agree well with the experimental data, with the best agreement occurring at 500 MeV. Results at 613 and 650 MeV are essentially the same. (New data from LAMPF at 650 MeV should be available in the near future.) The 500 and 800 MeV predictions are shown in Figs. 1 and 2 of Ref. 4. Predictions for the spin rotation function are also in good agreement with existing data.⁴ On the other hand, the KMT-IA predictions for $d\sigma/d\Omega$ display minima which are too deep for $E \leq 613$ MeV but are good at 800 and 1040 MeV. The analyzing powers and spin rotation predictions are poor at all energies; however, second order KMT-IA predictions that include electromagnetic spin orbit contributions¹⁵ are in better agreement with the data at 800 MeV (Ref. 16) than that shown by the dashed curves in Fig. 2 of Ref. 4.

Comparison of the RIA with the results of Dirac phenomenology¹ reveals several interesting features. First, the reactive content, as measured by the total reaction cross

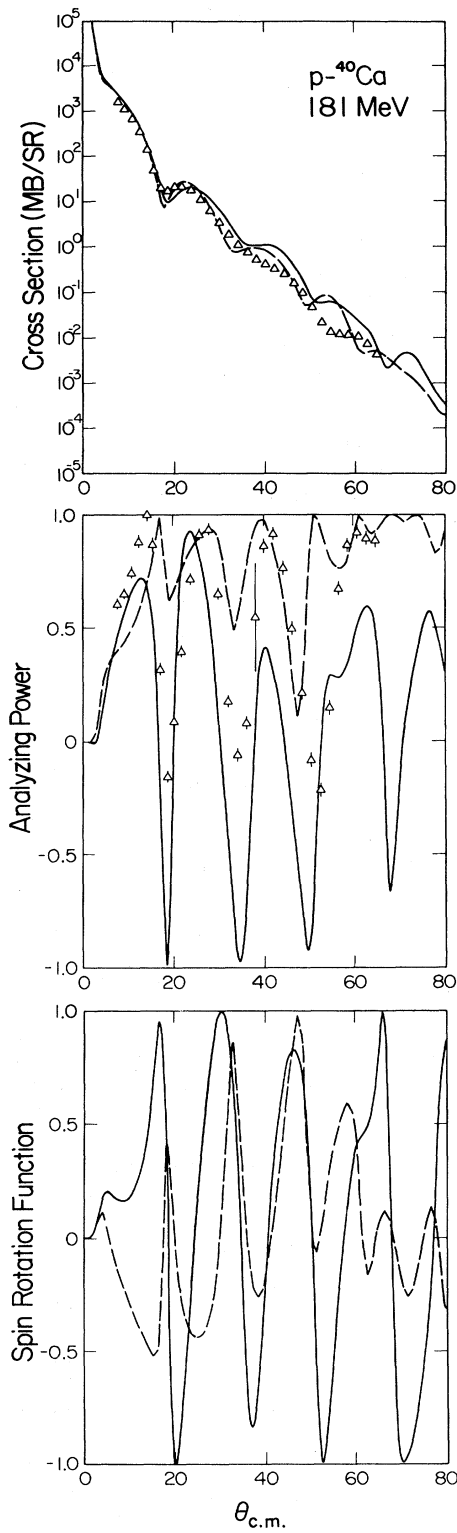


FIG. 1. The calculated cross section, analyzing power, and spin rotation function for $p + {}^{40}\text{Ca}$ at 181 MeV with use of the relativistic impulse approximation (solid curve), and the nonrelativistic impulse approximation (dashed curve).

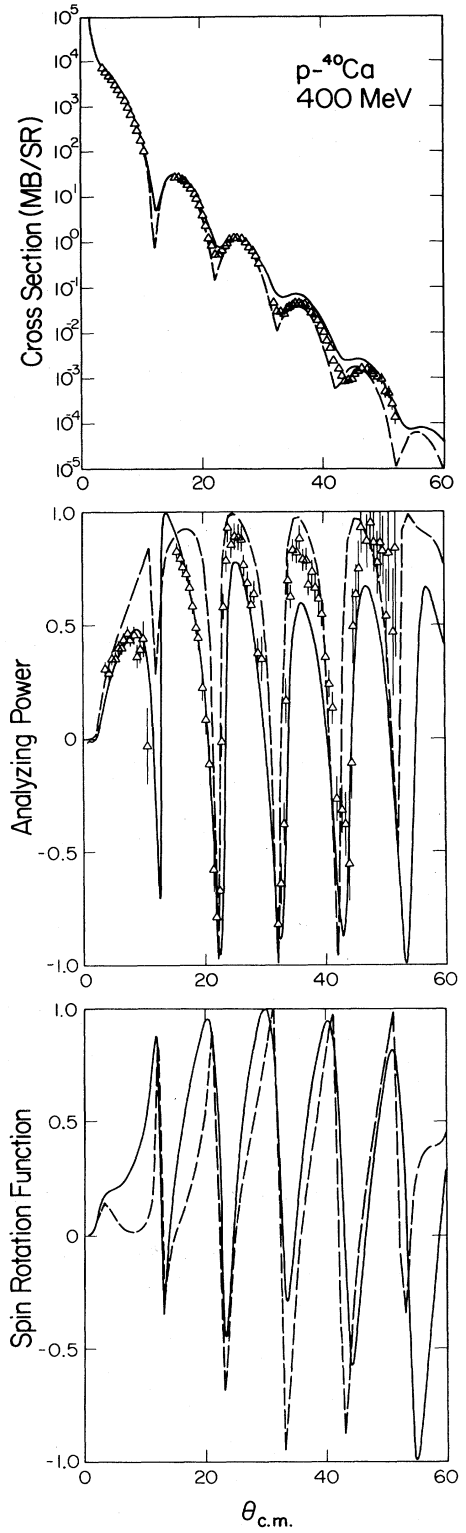
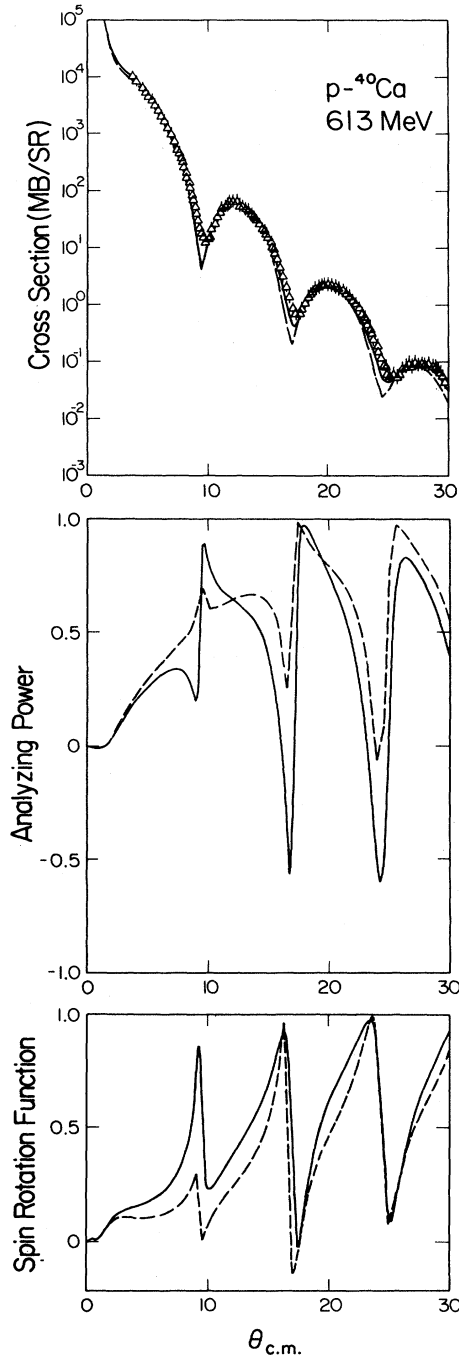


FIG. 2. Same as Fig. 1 for $p + {}^{40}\text{Ca}$ at 400 MeV.

FIG. 3. Same as Fig. 1 for $p+^{40}\text{Ca}$ at 613 MeV.

section, is well reproduced by the RIA. Phenomenological and RIA σ_R agree to within 1% at 300 MeV and above; at 181 MeV the difference is 7%. This agreement is substantially better than that obtained with KMT-IA calculations.¹⁷ The ratio of the volume integrals of the real vector to scalar potentials, a quantity well determined by the phenomenology, agrees to within 5% at 300 MeV and above; the values at 181 MeV differ by 7%. The rms radii of the RIA real and imaginary scalar and vector potentials are within 10% of

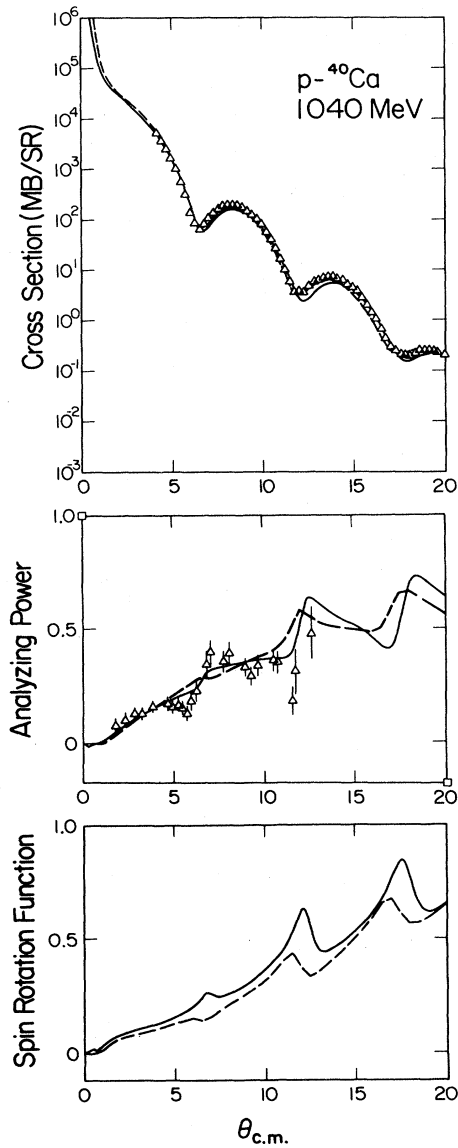
FIG. 4. Same as Fig. 1 for $p+^{40}\text{Ca}$ at 1040 MeV. The RIA and NR IA cross sections are essentially equal.

TABLE I. Ratio of relativistic IA to phenomenological volume integrals.

T_L (MeV)	Vector		Scalar	
	Real	Imag.	Real	Imag.
181	1.20	1.35	1.11	1.29
300	1.01	0.89	0.96	0.76
400	0.99	0.55	0.96	0.38
500	0.99	0.66	0.97	0.47
800	0.82	0.79	0.77	0.56

the corresponding phenomenological values at every energy. Comparing the volume integrals of phenomenological and RIA vector and scalar potentials provides another measure of the validity of the IA. Table I gives RIA to Dirac phenomenological volume integral ratios.¹ The agreement for the real potentials is very good in general except at 181 and 800 MeV and is substantially better than for the imaginary potentials. The largest discrepancy, around 300–500 MeV, for the imaginary potentials, mainly reflects differences in the central strengths of the imaginary RIA and phenomenological potentials. These results clearly indicate that similar studies of the energy dependence for other targets are called for, and such studies are in progress.

In this paper we have examined in detail the energy dependence of the relativistic impulse approximation for $p + {}^{40}\text{Ca}$ elastic scattering throughout the intermediate energy range. We find that the RIA predictions are in good

agreement with all the elastic observables for $E \geq 400$ MeV, whereas the first order KMT-IA predictions for $d\sigma/d\Omega$ are adequate only above 800 MeV, and the spin observables are poorly reproduced at all energies. The failure of the RIA model at lower energies may be due to medium effects (not included in the RIA), which have been shown to be important in explaining the Dirac phenomenology at lower energies.⁵ These effects will be the subject of future investigations.

We thank L. D. Miller and S. J. Wallace for discussions of the tensor contribution to the RIA. This research was supported in part by National Science Foundation Grants No. PHY 81-07397 and No. PHY 81-07395 and the U.S. Department of Energy. One of us (B.D.S) acknowledges a fellowship from the Alfred P. Sloan Research Foundation.

-
- ¹B. C. Clark, S. Hama, and R. L. Mercer, in *The Interaction Between Medium Energy Nucleons in Nuclei-1982*, edited by H. O. Meyer, AIP Conf. Proc. No. 97 (American Institute of Physics, New York, 1983), p. 260.
- ²J. A. McNeil, J. Shepard, and S. J. Wallace, Phys. Rev. Lett. 50, 1439 (1983).
- ³J. Shepard, J. A. McNeil, and S. J. Wallace, Phys. Rev. Lett. 50, 1443 (1983).
- ⁴B. C. Clark, S. Hama, R. L. Mercer, L. Ray, and B. D. Serot, Phys. Rev. Lett. 50, 1644 (1983).
- ⁵M. R. Anastasio, L. S. Celenza, and C. M. Shakin, Phys. Rev. C 23, 2606 (1981).
- ⁶J. A. McNeil, L. Ray, and S. J. Wallace, Phys. Rev. C 27, 2123 (1981).
- ⁷C. J. Horowitz and B. D. Serot, Nucl. Phys. A368, 503 (1981).
- ⁸S. J. Wallace (private communication). Calculations including the

tensor term show that this effect is negligible for the cases considered here.

- ⁹R. A. Arndt (private communication).
- ¹⁰L. G. Arnold, B. C. Clark, R. L. Mercer, and P. Schwandt, Phys. Rev. C 23, 1949 (1981).
- ¹¹D. Hutcheon *et al.* (private communication).
- ¹²T. Bauer *et al.* (unpublished). See G. Bruge, Saclay Report No. DPh-N/ME/78-1, 1978 (unpublished).
- ¹³G. Alkharov *et al.*, Nucl. Phys. A274, 443 (1976).
- ¹⁴L. Ray, Phys. Rev. C 19, 1855 (1979).
- ¹⁵Agreement of the RIA with experiment is slightly improved by including the effect of the anomalous magnetic moment of the projectile.
- ¹⁶Ray, Ref. 1, p. 121.
- ¹⁷L. Ray, Phys. Rev. C 20, 1857 (1979).